PCCP

PAPER

View Article Online
View Journal | View Issue

Cite this: *Phys. Chem. Chem. Phys.*, 2019, **21**, 10955

The metallo-formate anions, $M(CO_2)^-$, M = Ni, Pd, Pt, formed by electron-induced CO_2 activation

Gaoxiang Liu, [a] Sandra M. Ciborowski, [a] Zhaoguo Zhu,[a] Yinlin Chen, [a] Xinxing Zhang[b] and Kit H. Bowen*[a]

Received 5th April 2019,
Accepted 10th May 2019

DOI: 10.1039/c9cp01915d

rsc.li/pccp

The metallo-formate anions, $M(CO_2)^-$, M = Ni, Pd, and Pt, were formed by electron-induced CO_2 activation. They were generated by laser vaporization and characterized by a combination of mass spectrometry, anion photoelectron spectroscopy, and theoretical calculations. While neutral transition metal atoms are normally unable to activate CO_2, the addition of an excess electron to these systems led to the formation of chemisorbed anionic complexes. These are covalently bound, formate-like anions, in which their CO_2 moieties are significantly reduced. In addition, we also found evidence for an unexpectedly attractive interaction between neutral Pd atoms and CO_2.

Introduction

The activation of carbon dioxide underpins its chemistry. Since the carbon atom in CO_2 is in its highest oxidation state, the activation of CO_2 inevitably involves reducing it, and that implies CO_2 accepting some degree of negative charge. Accomplishing this, however, requires at least a partial bending of CO_2. The CO_2^- anion that results from CO_2 having accepted a full negative charge is metastable; the electron affinity of CO_2 is −0.6 eV. While some studies have dealt with free carbon dioxide anions, most have focused on anionic complexes consisting of CO_2 and various other atoms and molecules.[1–43] Anion photoelectron studies of N-heterocycle-CO_2 heterogeneous anionic dimers by Kim *et al.* showed significant covalent character in their intermolecular bond.[6,7] Subsequent work by Johnson *et al.*[8] and by ourselves[9] added additional dimensions to this topic. In all cases, however, the CO_2 moieties were found to be partially negatively-charged and bent. Infrared photodissociation studies of transition metal–CO_2 anionic complexes by Weber *et al.* further explored this topic.[10–23] Both electrostatically-bound, metal atom-multiple CO_2 anionic complexes (physisorption) and covalently-bound, metal atom-multiple CO_2 anionic complexes (chemisorption) were found. In the latter cases, the CO_2 moieties were partially bent and had accepted some significant portion of the negative charge, while in the former cases, the CO_2 were only very slightly bent, suggesting insignificant CO_2 activation. Calculations implied that the metal atoms were far away from the CO_2 moieties in the neutral complexes, and that their CO_2 moieties were structurally identical to isolated CO_2 molecules. Subsequent work in our laboratory measured the anion photoelectron spectra of copper–, silver–, and gold–CO_2 anionic dimers, finding only physisorption in the case of silver, *i.e.*, $Ag^-(CO_2)$, only chemisorption in the case of copper, *i.e.*, $Cu(CO_2)^-$, and both physisorbed and chemisorbed isomers for gold, *i.e.*, $Au^-(CO_2)$ and $Au(CO_2)^-$, respectively.[24]

Here, we present our study of the Group 10 transition metal–CO_2 anionic complexes: $[Ni(CO_2)]^-$, $[Pd(CO_2)]^-$, and $[Pt(CO_2)]^-$, using anion photoelectron spectroscopy and theoretical calculations. In contrast to our previous work with the Group 11 coinage (s^1) metals, the Group 10 metals adopt richer outer electron shell configurations (d^8s^2 for Ni, d^{10} for Pd, and d^9s^1 for Pt) with significantly greater prospects for complex chemical bonding. Indeed, strong evidence for chemisorption was found in all three of the Group 10 metal–CO_2 anionic complexes studied here, implying that Ni^-, Pd^- and Pt^- all activated CO_2 to form $Ni(CO_2)^-$, $Pd(CO_2)^-$, and $Pt(CO_2)^-$, respectively. Thus, all three of these Group 10 metal anions were seen to be able to both reduce and activate CO_2.

Methods

Experimental

Anion photoelectron spectroscopy is conducted by crossing a beam of mass-selected negative ions with a fixed-frequency photon beam and energy-analyzing the resultant photodetached electrons. The photodetachment process is governed by the energy-conserving relationship: $h\nu$ = EBE + EKE, where $h\nu$ is the photon energy, EBE is the electron binding (photodetachment transition) energy, and EKE is the electron kinetic energy. Our apparatus consists of a laser vaporization cluster anion source,

[a] *Department of Chemistry, Johns Hopkins University, Baltimore, Maryland 21218, USA. E-mail: kbowen@jhu.edu*
[b] *Key Laboratory of Advanced Energy Materials Chemistry (Ministry of Education), College of Chemistry, Nankai University, Tianjin 300071, China*

a time-of-flight mass spectrometer, a Nd:YAG photodetachment laser, and a magnetic bottle electron energy analyzer.[44] The photoelectron spectrometer resolution is ~35 meV at EKE = 1 eV. The third harmonic output of a Nd:YAG laser (355 nm) was used to photodetach electrons from mass-selected M^- and $[M(CO_2)]^-$ anions, where M = Ni, Pd, Pt. Photoelectron spectra were calibrated against the well-known atomic transitions of atomic Cu^-.[45] The $[M(CO_2)]^-$ (M = Ni, Pd, Pt) anion complexes were generated in a laser vaporization ion source. It consisted of rotating, translating nickel, palladium, or platinum rods, which were ablated with second harmonic (532 nm) photon pulses from a Nd:YAG laser, while 10%/90% He/CO_2 gas mixtures at 60 psi were expanded from a pulsed valve over the rods.

Theoretical

Density functional theory calculations were performed with the ORCA computational chemistry software package.[46] All calculations were carried out with the B3LYP functional[47] with the D3 dispersion correction[48] and the RIJCOSX approximation.[49] The Ahlrichs Def2 basis sets were used throughout our calculations.[50] For geometry optimization, Def2-TZVP and auxiliary Def2-TZVP/J basis sets[51] were chosen for carbon, oxygen and nickel atoms; the Stuttgart effective core potential SDD[52] and ECP basis set Def2-TZVP|Def2-TZVP/J were used for palladium and platinum atoms. The potential energy surfaces of neutral Ni, Pt–CO_2 along the M–C coordinate were computed by scanning the M–C bond length with a step width of 0.1 Å, while relaxing the rest of the cluster. Single-point calculations were then improved with Def2-QZVPP|Def2-QZVPP/J basis sets and all-electron relativistic calculations (ZORA). The structure of neutral $PdCO_2$ was also checked using the PBE0 and M06-L functionals.[53] The vertical detachment energy (VDE) is the energy difference between the ground state anion and its corresponding neutral at the geometry of the anion, *i.e.*, these are vertical photodetachment transitions. The adiabatic detachment energy (ADE) is the energy difference between the lowest energy, relaxed geometry of the anion and the relaxed geometry of a structurally similar isomer (nearest minimum) of its neutral counterpart. The adiabatic electron affinity (EA) is the energy difference between the lowest energy, relaxed geometry of the anion and the relaxed geometry of the lowest energy isomer (the global minimum) of its neutral counterpart. When the nearest local minimum and the global minimum are one and the same, ADE = EA. In this work, we calculated ADE values. In the systems studied here, there is only one credible minimum for the neutral species, and it is therefore the global minimum. For that reason, we report ADE values as EA values here. Also, note that since the Franck–Condon principle governs which spectral features are seen within its anion-to-neutral wavefunction overlap window, there is often a correspondence between the lowest EBE transition observed experimentally and the properly calculated ADE value. Franck–Condon simulation was performed for the $PdCO_2^-$ spectrum. This simulation, however, was not practical for $NiCO_2^-$ and $PtCO_2^-$ due to the large structural changes between anions and neutrals. Frequency calculations were performed to verify that no imaginary frequencies existed for any of the optimized structures.

Results and discussion

The photoelectron spectra of $[M(CO_2)]^-$ (M = Ni, Pd, Pt) are presented in Fig. 1. For comparison, the atomic anion photoelectron spectra of Ni^-, Pd^-, and Pt^- are also presented above each $[M(CO_2)]^-$ spectrum there. In the anionic complexes, $[M(CO_2)]^-$, the CO_2 moiety can be either physisorbed or chemisorbed to M^-. For physisorbed complexes, the interaction between M^- and CO_2 is weak; they can be considered to be M^- anions "solvated" by CO_2 molecules, *i.e.*, $M^-(CO_2)$. In physisorbed anion-molecule complexes such as these, their M^- anion

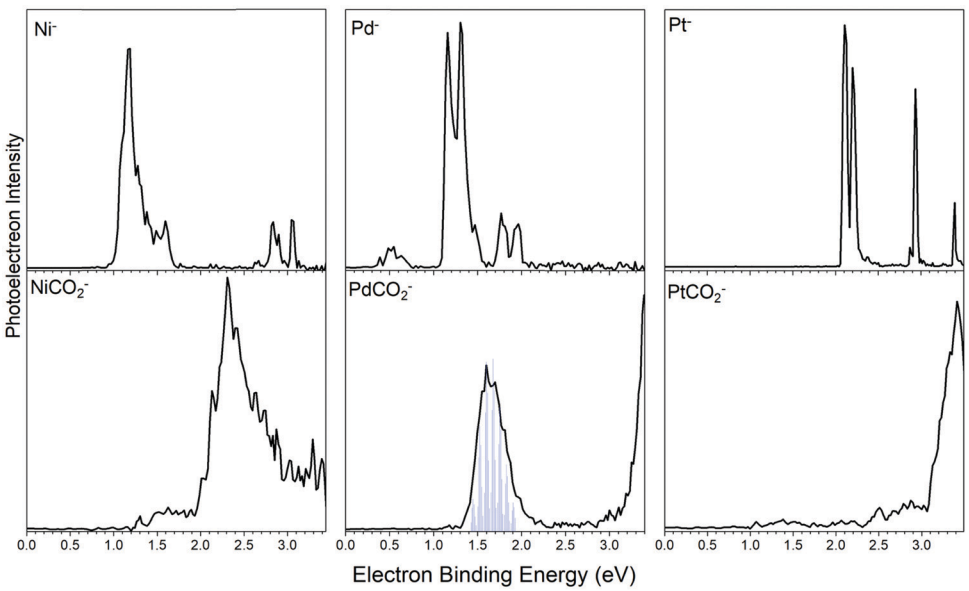

Fig. 1 Anion photoelectron spectra of Ni^- and $NiCO_2^-$, Pd^- and $PdCO_2^-$, and Pt^- and $PtCO_2^-$. The vertical lines in the $PdCO_2^-$ spectrum represent Franck–Condon simulated vibrational progression.

moieties act as chromophores for photodetachment, with the resulting photoelectron spectra closely resembling the photoelectron spectral patterns of M^-, just shifted to higher electron binding energies (EBE) with their spectral features slightly broadened.[54,55] These shifts are typically a few tenths of an eV, corresponding approximately to ion-solvation stabilization energies. This spectral behavior provides a distinctive spectroscopic signature for physisorbed (solvated) anion complexes. The photoelectron spectra of $[Ni(CO_2)]^-$, $[Pd(CO_2)]^-$, and $[Pt(CO_2)]^-$, however, do not exhibit this behavior in relation to their atomic anion photoelectron spectra, *i.e.*, Ni^-, Pd^-, and Pt^-. They are not physisorbed species. Moreover, their spectral shifts are far too large to be due to weak, solvation-like interactions. The spectral shifts between the lowest EBE features of the atomic anions and those of their corresponding anionic complexes are about an electron volt. The anionic complexes studied here, *i.e.*, $[Ni(CO_2)]^-$, $[Pd(CO_2)]^-$, and $[Pt(CO_2)]^-$, are chemisorbed complexes, *i.e.*, $NiCO_2^-$, $PdCO_2^-$, and $PtCO_2^-$. Significant chemical interactions have occurred, resulting in bonds between the metal atoms and their CO_2 moieties.

Energetic parameters can also be determined from the spectra. When there is sufficient Franck–Condon overlap between the ground state of the anion and the ground state of the neutral, and when vibrational hot bands are absent, the threshold EBE (E_T) is the value of the electron affinity (EA). The E_T in $PdCO_2^-$ spectrum can be determined definitively. For $NiCO_2^-$ and $PdCO_2^-$, however, the relatively weak, shelf-like features on the low EBE side of the major peaks are likely hot bands. Thus, the E_T values for those two systems were determined by extrapolating the low EBE sides of their major peaks to baseline. In all three anionic complexes, the EBE values of the intensity maxima in their major peaks are their vertical detachment energy (VDE) values, corresponding to the transitions that have maximum Franck–Condon overlap between the ground electronic states of the anionic complexes and their neutral counterparts. The onset of the higher EBE feature in $PdCO_2^-$ spectrum is due to the vertical photodetachment transition from the ground state anion to its neutral counterpart in its first excited electronic state. The EA and VDE values of $NiCO_2^{0/-}$, $PdCO_2^{0/-}$, and $PtCO_2^{0/-}$ are listed in Table 1.

A synergy between theoretical calculations and anion photoelectron spectroscopy can provide insights into the structures, energetics and the nature of chemical bond of the investigated clusters.[55–61] The calculated structures of the anionic complexes and their corresponding neutrals are presented in Fig. 2. The first row shows the geometries of the anionic complexes along with their respective HOMOs, while the second row provides the geometries of their neutral counterparts. The M–C bond length (Å), the C–O bond length (Å), and the O–C–O bond angle (in degrees) are shown for each case. For the chemisorption species, $NiCO_2^-$, $PdCO_2^-$, and $PtCO_2^-$, the M–C bond lengths are 2.01 Å, 2.03 Å, and 2.02 Å, respectively, suggesting the formation of single bonds between M and C in all cases. The CO_2 moiety is significantly bent in all three anionic. complexes, with an O–C–O bond angle of 138.26° for $NiCO_2^-$, 140.62° for $PdCO_2^-$ and 136.34° for $PtCO_2^-$, respectively. A natural population analysis shows that the CO_2 moieties in $NiCO_2^-$, $PdCO_2^-$, and $PtCO_2^-$ have negative charges of $-0.75\ e$, $-0.59\ e$, and $-0.67\ e$, respectively. Thus, the CO_2 moiety has been significantly reduced in all of these anionic complexes. The O–C–O bond angles in all three systems are similar one another, as are the negative charges on their CO_2 moieties. The fact that they are not completely synchronized is likely due to the natural population analysis (NPA) being less reliable than the structural calculations. For the three anionic complexes, the C–O bond lengths are all between 1.22–1.23 Å, which is longer than the 1.16 Å C–O bond length in isolated CO_2 (1.16 Å). This implies that when negative charge is transferred to the CO_2 moiety, the C–O bond is elongated and weakened. Thus, $NiCO_2^-$, $PdCO_2^-$, and $PtCO_2^-$ all share a metallo-formate geometry. Furthermore, they are structurally quite similar in terms of M–C bond length, C–O bond length and O–C–O bond angle. Note that based on the calculated structures and charge distributions, Pd^- seems to have the weakest interaction with CO_2 of all three metal anions, although Pd has the lowest electron affinity which is expected to facilitate the charge transfer to the CO_2 moiety. One possible reason for Pd^- being the outlier is its electron configuration, $d_{10}s$, which is different to that of Ni^- and Pt^-, d_9s_2. The calculated EA and VDE values are listed in Table 1 along with their corresponding experimental values. Excellent agreement between experimental and theoretical values, is seen for all three anionic complexes, validating the geometry optimizations shown in Fig. 2.

In neutral $NiCO_2$ and $PtCO_2$, the metal atom is far away from CO_2. Also, their CO_2 moieties are structurally identical to an isolated CO_2 molecule. The potential energy surfaces of neutral $NiCO_2$ and $PtCO_2$ seem to show a shallow energy well at a M–C bond length of around 2.0 Å, but the energies of these local minima are higher than when CO_2 is far away (Fig. 3). The repulsive part of the neutral surfaces occurs at a M–C bond length less than 1.9 Å. Since $NiCO_2^-$ and $PtCO_2^-$ have a M–C bond length of 2.01 and 2.02 Å, respectively, the repulsive part of each neutral surface is not accessed during the vertical photodetachment process. The structural parameters show that there is little interaction between the neutral atoms of Ni and Pt and CO_2, which is as expected based on our previous research.[24] Surprisingly, however, the optimized neutral $PdCO_2$ structure shows incipient chemisorption character, that while much weaker than in its $PdCO_2^-$ anionic counterpart, is significantly stronger than the physisorption interactions seen in neutral $NiCO_2$ and $PtCO_2$. In neutral $PdCO_2$, the Pd–C bond length is 2.31 Å, which is characteristic of a metal–carbon bond. The CO_2 moiety is noticeably bent, with the O–C–O bond angle being 163.42°. The NPA analysis shows the CO_2 moiety as possessing a negative charge of $-0.16\ e$, indicating a degree of charge transfer

Table 1 Experimental and theoretical EA and VDE values for MCO_2 and MCO_2^-, M = Ni, Pd, Pt, respectively. All values are in eV

	EA (expt/theo.)	VDE (expt/theo.)
$NiCO_2^{0/-}$	1.9/1.86	2.33/2.31
$PdCO_2^{0/-}$	1.3/1.10	1.60/1.57
$PtCO_2^{0/-}$	3.0/2.81	3.43/3.37

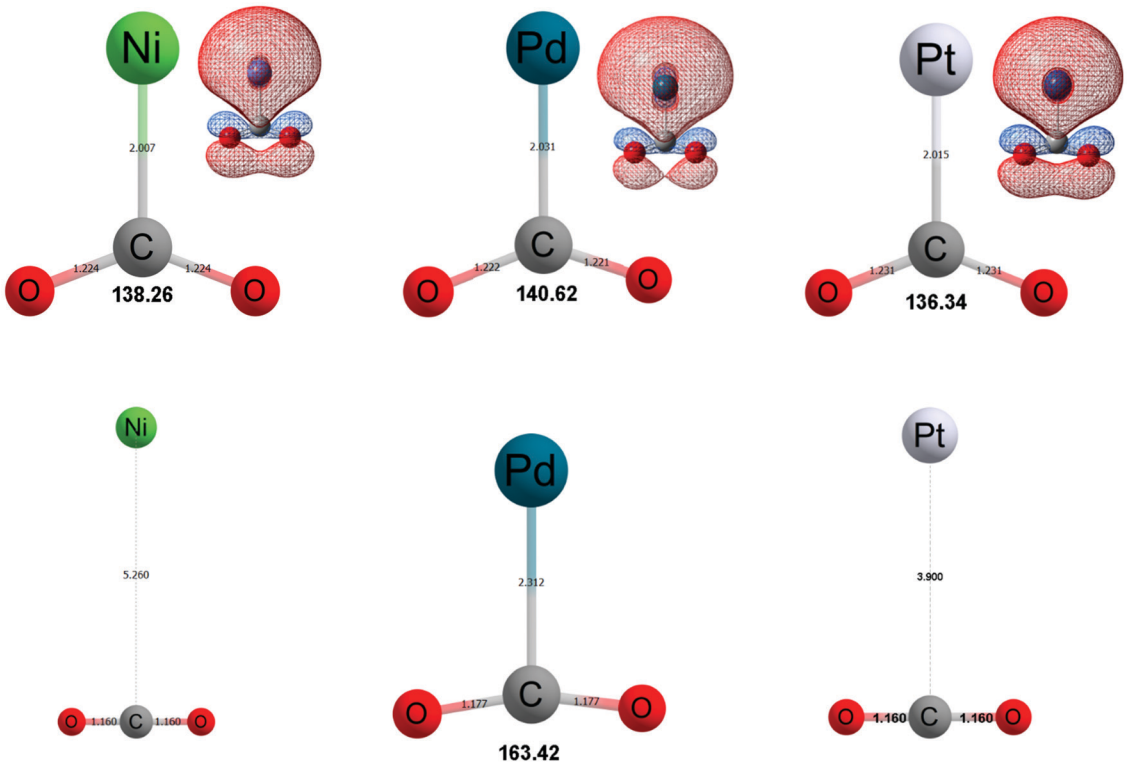

Fig. 2 Calculated structures of $NiCO_2^-$, $PdCO_2^-$, $PtCO_2^-$ (first row) and $NiCO_2$, $PdCO_2$, $PtCO_2$ (second row). The HOMOs of the anionic complexes are also presented.

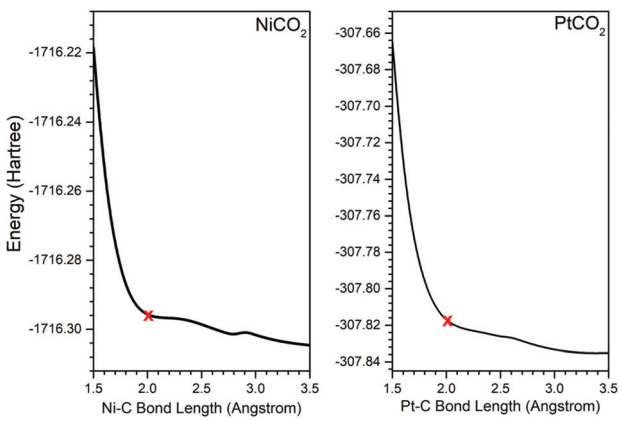

Fig. 3 The potential energy surfaces of neutral $NiCO_2$ and $PtCO_2$ with respect to the M–C bond length. The red crosses represent the M–C bond length of optimized anionic $NiCO_2^-$ and $PtCO_2^-$.

between neutral Pd and CO_2. The neutral $PdCO_2$ structure was also verified using the PBE0 and M06-L functionals. Both functionals yielded the same $PdCO_2$ structure as the B3LYP one. In addition, the Franck–Condon simulated spectrum of $PdCO_2^-$ reproduces the experimental one (Fig. 1), offering a further validation of the neutral $PdCO_2$ structure. Taken together, these features suggest that CO_2 can be activated by a single neutral Pd atom.

In order to provide further insight into the nature of the bonding in neutral $PdCO_2$, we analyzed its molecular orbitals. In most cases, the molecular orbitals of neutral $M(CO_2)$ species are composed of atomic orbitals of M and molecular orbitals of CO_2, which are essentially independent of one another. The molecular orbitals of neutral $PtCO_2$ (HOMO to HOMO−8) are presented on the left side of Fig. 4, and they provide typical examples of the molecular orbitals in neutral MCO_2 species. The absence of wavefunction overlap between the M and CO_2 moieties is consistent with a lack of interaction between neutral M atoms and CO_2 moieties. In the case of neutral $PdCO_2$, most of its molecular orbitals can also be viewed as independent atomic orbitals of Pd and molecular orbitals of CO_2. However, this is not the case for all orbital interactions between Pd and CO_2.

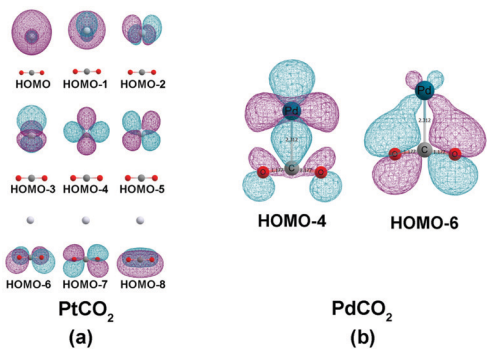

Fig. 4 Selected molecular orbitals of neutral (a) $PtCO_2$ and (b) $PdCO_2$. The overlap between the metal atomic orbitals and the CO_2 molecular orbitals is barely present in neutral $PtCO_2$, but is significant in neutral $PdCO_2$.

The HOMO−4 and HOMO−6 orbitals, seen on the right side of Fig. 3, clearly result from the combination of Pd atomic orbitals and CO_2 molecular orbitals. There, one observes significant interaction, *i.e.*, overlap, between some of the orbitals of Pd and CO_2. For HOMO−4, the interaction is mainly between the Pd d_{z^2} orbital and the B_1 orbital of bent CO_2. For HOMO−6, the interaction is through the overlap between Pd d_{xy} orbital and the B_2 orbital of bent CO_2. The wavefunction overlap between these Pd atomic and CO_2 molecular orbitals is likely the reason for the weak binding interaction and the partial charge transfer between neutral Pd atom and CO_2. Although we are unaware of corroborating experimental evidence for their weak binding, our calculations imply a neutral $PdCO_2$ bond dissociation energy of 0.85 eV. For comparison, the bond dissociation energy of the $PdCO_2^-$ anionic complex is predicted to be 1.78 eV.

Conclusion

This combined anion photoelectron spectroscopic and computational study characterized the metallo-formate anions, $M(CO_2)^-$, where M = Ni, Pd, and Pt, and demonstrated that the addition of an excess electron led to significant CO_2 reduction in these systems. While neutral transition metals are normally incapable of reducing CO_2, we found evidence of an unusual attractive interaction between neutral Pd and CO_2.

Conflicts of interest

The authors declare no competing financial interest.

Acknowledgements

This material is based on work supported by the U.S. National Science Foundation under Grant No. CHE-1664182 (KHB).

References

1 R. N. Compton, P. W. Reinhardt and C. D. Cooper, *J. Chem. Phys.*, 1975, **63**, 3821.
2 M. Knapp, O. Echt, D. Kreisle, T. D. Mark and E. Recknagel, *Chem. Phys. Lett.*, 1986, **126**, 225.
3 S. T. Arnold, J. V. Coe, J. G. Eaton, C. B. Freidhoff, L. H. Kidder, G. H. Lee, M. R. Manaa, K. M. McHugh, D. Patel-Misra, H. W. Sarkas, J. T. Snodgrass and K. H. Bowen, in *Proceedings of the Enrico Fermi International School of Physics, CVII Course, Varenna*, ed. G. Scoles, North-Holland, Amsterdam, 1989, pp. 467–490.
4 C. E. Klots, *J. Chem. Phys.*, 1979, **71**, 4172.
5 T. Tsukuda and T. Nagata, *J. Phys. Chem. A*, 2003, **107**, 8476.
6 S. Y. Han, I. Chu, J. H. Kim, J. K. Song and S. K. Kim, *J. Chem. Phys.*, 2000, **113**, 596.
7 S. H. Lee, N. Kim, D. G. Ha and S. K. Kim, *J. Am. Chem. Soc.*, 2008, **130**, 16241.
8 M. Z. Kamrath, R. A. Relph and M. A. Johnson, *J. Am. Chem. Soc.*, 2010, **132**, 15508.
9 J. D. Graham, A. M. Buytendyk, Y. Wang, S. K. Kim and K. H. Bowen, *J. Chem. Phys.*, 2015, **142**, 234307.
10 J. M. Weber, *Int. Rev. Phys. Chem.*, 2014, **33**, 489.
11 H. Schneider, A. D. Boese and J. M. Weber, *J. Chem. Phys.*, 2005, **123**, 074316.
12 A. D. Boese, H. Schneider, A. N. Glöß and J. M. Weber, *J. Chem. Phys.*, 2005, **122**, 154301.
13 B. J. Knurr and J. M. Weber, *J. Am. Chem. Soc.*, 2012, **134**, 18804.
14 B. J. Knurr and J. M. Weber, *J. Phys. Chem. A*, 2013, **117**, 10764.
15 B. J. Knurr and J. M. Weber, *J. Phys. Chem. A*, 2014, **118**, 4056.
16 B. J. Knurr and J. M. Weber, *J. Phys. Chem. A*, 2014, **118**, 10246.
17 B. J. Knurr and J. M. Weber, *J. Phys. Chem. A*, 2014, **118**, 8753.
18 M. C. Thompson, J. Ramsay and J. M. Weber, *J. Phys. Chem. A*, 2017, **121**, 7537.
19 M. C. Thompson, Leah G. Dodson and J. M. Weber, *J. Phys. Chem. A*, 2017, **121**, 4132.
20 M. C. Thompson, J. Ramsay and J. M. Weber, *Angew. Chem., Int. Ed.*, 2016, **55**, 15171.
21 L. G. Dodson, M. C. Thompson and J. M. Weber, *J. Phys. Chem. A*, 2018, **122**, 2983.
22 M. C. Thompson and J. M. Weber, *J. Phys. Chem. A*, 2018, **122**, 3772.
23 L. G. Dodson, M. C. Thompson and J. M. Weber, *Annu. Rev. Phys. Chem.*, 2018, **69**, 231.
24 X. Zhang, E. Lim, S. K. Kim and K. H. Bowen, *J. Chem. Phys.*, 2015, **143**, 174305.
25 N. Kim, *Bull. Korean Chem. Soc.*, 2015, **34**, 2247.
26 M. J. DeLuca, B. Niu and M. A. Johnson, *J. Chem. Phys.*, 1988, **88**, 5857.
27 S. H. Fleischman and K. D. Jordan, *J. Phys. Chem.*, 1987, **91**, 1300.
28 T. Tsukuda, M. A. Johnson and T. Nagata, *Chem. Phys. Lett.*, 1977, **268**, 429.
29 J. W. Shin, N. I. Hammer, M. A. Johnson, H. Schneider, A. Glöß and J. M. Weber, *J. Phys. Chem. A*, 2015, **109**, 3146.
30 D. W. Arnold, S. E. Bradforth, E. H. Kim and D. M. Neumark, *J. Chem. Phys.*, 1995, **102**, 3493.
31 G. Markovich, R. Giniger, M. Levin and O. Cheshnovsky, *Z. Phys. D: At., Mol. Clusters*, 1991, **20**, 69.
32 D. W. Arnold, S. E. Bradforth, E. H. Kim and D. M. Neumark, *J. Chem. Phys.*, 1992, **97**, 9468.
33 D. W. Arnold, S. E. Bradforth, E. H. Kim and D. M. Neumark, *J. Chem. Phys.*, 1995, **102**, 3510.
34 A. Muraoka, Y. Inokuchi, N. I. Hammer, J. W. Shin, M. A. Johnson and T. Nagata, *J. Phys. Chem. A*, 2009, **113**, 8942.
35 K. Hiraoka and S. Yamabe, *J. Chem. Phys.*, 1992, **97**, 643.
36 K. Sudoh, Y. Matsuyama, A. Muraoka, R. Nakanishi and T. Nagata, *Chem. Phys. Lett.*, 2006, **433**, 10.
37 T. Sanford, S. Y. Han, M. A. Thompson, R. Parson and W. C. Lineberger, *J. Chem. Phys.*, 2005, **122**, 054307.
38 R. F. Höckendorf, K. Fischmann, Q. Hao, C. v. d. Linde, O. P. Balaj, C. K. Siu and M. K. Beyer, *Int. J. Mass Spectrom.*, 2013, **354**, 175.
39 A. Akhgarnusch, R. F. Hoeckebdorf, Q. Hao, K. P. Jaeger, C. K. Siu and M. K. Beyer, *Angew. Chem., Int. Ed.*, 2013, **53**, 9327.

40 A. Akhgarnusch and M. K. Beyer, *Int. J. Mass Spectrom.*, 2014, **365**, 295.
41 R. Oh, E. Lim, X. Zhang, J. Heo, K. H. Bowen and S. K. Kim, *J. Chem. Phys.*, 2017, **146**, 134304.
42 X. Zhang, G. Liu, K. Meiwes-Broer, G. Gantefçr and K. Bowen, *Angew. Chem., Int. Ed.*, 2016, **55**, 9644.
43 J. D. Graham, A. M. Buytendyk, X. Zhang, S. K. Kim and K. H. Bowen, *J. Chem. Phys.*, 2015, **143**, 184315.
44 G. Liu, S. M. Ciborowski and K. H. Bowen, *J. Phys. Chem. A*, 2017, **121**, 5817.
45 J. Ho, K. M. Ervin and W. C. Lineberger, *J. Chem. Phys.*, 1990, **93**, 6987.
46 F. Neese, *WIREs Comput. Mol. Sci.*, 2012, **2**, 73.
47 (*a*) A. D. Becke, *Phys. Rev. A: At., Mol., Opt. Phys.*, 1988, **38**, 3098; (*b*) A. D. Becke, *J. Chem. Phys.*, 1993, **98**, 5648.
48 (*a*) C. Lee, W. Yang and R. G. Parr, *Phys. Rev. B: Condens. Matter Mater. Phys.*, 1988, **37**, 785; (*b*) R. Krishnan, J. S. Binkley, R. Seeger and J. A. Pople, *J. Chem. Phys.*, 1980, **72**, 65.
49 S. Grimme, J. Antony, S. Ehrlich and H. A. Krieg, *J. Chem. Phys.*, 2010, **132**, 154104.
50 F. Neese, F. Wennmohs, A. Hansen and U. Becker, *Chem. Phys.*, 2008, **356**, 98.
51 (*a*) F. Weigend and R. Ahlrichs, *Phys. Chem. Chem. Phys.*, 2005, **7**, 3297; (*b*) F. Weigend, *Phys. Chem. Chem. Phys.*, 2006, **8**, 1057.
52 D. Andrae, U. Häußermann, M. Dolg, H. Stoll and H. Preuß, *Theor. Chim. Acta*, 1990, **77**, 123.
53 (*a*) C. Adamo and V. Barone, *J. Chem. Phys.*, 1994, **110**, 6158–6170; (*b*) J. P. Perdew, K. Burke and M. Ernzerhof, *Phys. Rev. Lett.*, 1997, **77**, 3865; (*c*) Y. Zhao and D. G. Truhlar, *J. Phys. Chem. A*, 2006, **110**, 13126–13130; (*d*) Y. Zhao and D. G. Truhlar, *Theor. Chem. Acc.*, 2007, **120**, 215–241.
54 G. Liu, E. Miliordos, S. M. Ciborowski, M. Tschurl, U. Boesl, U. Heiz, X. Zhang, S. S. Xantheas and K. H. Bowen, *J. Chem. Phys.*, 2018, **149**, 221101.
55 G. Liu, Z. Zhu, S. M. Ciborowski, I. R. Ariyarathna, E. Miliordos and K. H. Bowen, *Angew. Chem., Int. Ed.*, 2019, **131**, DOI: 10.1002/anie.201903252.
56 X. Zhang, G. Liu, S. Ciborowski and K. Bowen, *Angew. Chem., Int. Ed.*, 2017, **56**, 9897.
57 K. A. Lundell, X. Zhang, A. I. Boldyrev and K. H. Bowen, *Angew. Chem., Int. Ed.*, 2017, **56**, 16593.
58 P. J. Robinson, G. Liu, S. Ciborowski, C. Martinez-Martinez, J. R. Chamorro, X. Zhang, T. M. McQueen, K. H. Bowen and A. N. Alexandrova, *Chem. Mater.*, 2017, **29**, 9892.
59 X. Zhang, G. Liu, S. Ciborowski and K. H. Bowen, *Angew. Chem., Int. Ed.*, 2017, **56**, 9897.
60 E. F. Belogolova, G. Liu, E. P. Doronina, S. Ciborowski, V. F. Sidorkin and K. H. Bowen, *J. Phys. Chem. Lett.*, 2018, **9**, 1284.
61 X. Zhang, I. A. Popov, K. A. Lundell, H. Wang, C. Mu, W. Wang, H. Schnöckel, A. I. Boldyrev and K. H. Bowen, *Angew. Chem., Int. Ed.*, 2018, **130**, 14256.

